ORIGINAL ARTICLE

Clinical features, treatment, and follow-up of OPPG and high-bone-mass disorders: LRP5 is a key regulator of bone mass

Na Ren[1] · Shanshan Lv[1] · Xiang Li[1] · Chong Shao[1] · Ziyuan Wang[1] · Yazhao Mei[1] · Wendi Yang[1] · Wenzhen Fu[1] · Yunqiu Hu[1] · Ling Sha[1] · Weiwei Hu[1] · Zhenlin Zhang[1] · Chun Wang[1]

Abstract

Summary Osteoporosis-pseudoglioma syndrome (OPPG) and LRP5 high bone mass (LRP5-HBM) are two rare bone diseases with opposite clinical symptoms caused by loss-of-function and gain-of-function mutations in *LRP5*. Bisphosphonates are an effective treatment for OPPG patients. LRP5-HBM has a benign course, and age-related bone loss is found in one LRP5-HBM patient.

Purpose *Low-density lipoprotein receptor-related protein 5* (*LRP5*) is involved in the canonical Wnt signaling pathway. The gain-of-function mutation leads to high bone mass (LRP5-HBM), while the loss-of-function mutation leads to osteoporosis-pseudoglioma syndrome (OPPG). In this study, the clinical manifestations, disease-causing mutations, treatment, and follow-up were summarized to improve the understanding of these two diseases.

Methods Two OPPG patients and four LRP5-HBM patients were included in this study. The clinical characteristics, biochemical and radiological examinations, pathogenic mutations, and structural analysis were summarized. Furthermore, several patients were followed up to observe the treatment effect and disease progress.

Results Congenital blindness, persistent bone pain, low bone mineral density (BMD), and multiple brittle fractures were the main clinical manifestations of OPPG. Complex heterozygous mutations were detected in two OPPG patients. The c.1455G > T mutation in exon 7 was first reported. During the follow-up, BMD of two patients was significantly improved after bisphosphonate treatment.

On the contrary, typical clinical features of LRP5-HBM included extremely high BMD without fractures, torus palatinus and normal vision. X-ray showed diffuse osteosclerosis. Two heterozygous missense mutations were detected in four patients. In addition, age-related bone loss was found in one LRP5-HBM patient after 12-year of follow-up.

Conclusion This study deepened the understanding of the clinical characteristics, treatment, and follow-up of OPPG and LRP5-HBM; expanded the pathogenic gene spectrum of OPPG; and confirmed that bisphosphonates were effective for OPPG. Additionally, it was found that Ala242Thr mutation could not protect LRP5-HBM patients from age-related bone loss. This phenomenon deserves further study.

Keywords High bone mass · *LRP5* · LRP5-HBM · OPPG · Osteoporosis · Wnt

Introduction

Low-density lipoprotein receptor-related protein 5 (LRP5) is a type I transmembrane receptor belonging to the LDL receptor family, composed of an extracellular domain, a membrane-spanning domain, and an intracellular domain [1]. The extracellular domain is a binding region that has extremely high affinity for the ligand, composed of four YWTD β-propellers, four EGF-like domains, and LDLR type A domains [2]. It acts as a coreceptor involved in Wnt signal transduction and consequential normal osteogenic

✉ Zhenlin Zhang
zhangzl@sjtu.edu.cn

✉ Chun Wang
wangchun66@sjtu.edu.cn

1 Department of Osteoporosis and Bone Disease, Shanghai Clinical Research Center of Bone Disease, Sixth People's Hospital Affiliated to Shanghai Jiao Tong University School of Medicine, Yishan Road 600, Shanghai 200233, China

activity of osteoblasts, reported to be one of the regulators of peak bone mass in vertebrates already [3]. It is the coreceptor of Frizzled and can be activated by proteins of the Wnt family, and then through a series of intracellular reactions, β-catenin was allowed to enter the nucleus and to modulate relative gene-transcription regulators, which is the Wnt canonical pathway [4]. In the aspect of osteogenesis, it is shown to strongly activates bone formation by enhancing cell commitment toward the bone lineage and the proliferation and differentiation of osteoblasts [2]. On the other hand, Dickkopf (DKK)1 and sclerostin (SOST), the natural antagonists of the Wnt pathway, can bind Kremen and LRP5 and block this canonical pathway, leading to the inhibition of bone formation moderately and maintenance of bone homeostasis finally [5].

LRP5 has already been identified to be associated with both osteoporosis-pseudoglioma syndrome (OPPG, OMIM 259,770) and LRP5 high bone mass (LRP5-HBM, OMIM 144,750), due to *LRP5* loss-of-function mutations and gain-of-function mutations, respectively [6, 7]. The failure of properly activating Wnt signaling in osteoblasts due to loss-of-function mutations may impaired bone formation. However, the weaken binding to DKK1 and SOST because of *LRP5* gain-of-function mutations reduces inhibitory effects on Wnt signaling, where osteoblast activity is increased and therefore bone formation is enhanced, which may be the cause of the high-bone-mass phenotype [7, 8].

OPPG is an autosomal recessive disorder characterized by severe juvenile-onset osteoporosis and congenital or juvenile-onset blindness [6]. Low bone mass is often found in early childhood and is usually accompanied by fragility fractures or malformations of the long bones and spine. However, some patients suffer from fractures as early as infancy [9, 10]. And patients suffer from blindness after birth [6]. Eye problems such as phthisis bulbi, retinal detachments, and falciform folds usually appear within a few days or 1–3 years after birth [11, 12].

In contrast, LRP5-HBM is a type of autosomal dominant bone disease, and its typical clinical characteristics of this disease include generalized high bone density; torus palatinus; and a wide, deep mandible [7]. Patients often show radiographically cortical thickening of diaphyses of long bones but usually little change of bone outer shape and dimensions, and osteosclerosis of ribs, clavicles, vertebrae, hip, metacarpals, and calvaria [13]. The most common facial changes are elongated mandible and torus palatinus, accounting for 61% and 41%, respectively [14]. Fortunately, this disease seems benign for no danger of fragile fractures and anemia, and sometimes, it is totally asymptomatic except for the imaging abnormalities [7]. However, there are some cases reported symptoms of neurological involvement such as trigeminal neuralgia, sensorineural hearing loss, partial visual field defects, mild facial paralysis, chronic occipital headache,

and type I Chiari [15, 16], speculated as the related brain tissue and nerve compression by the hyperostotic bone [17]. It is estimated that cranial nerve deficits and/or other neurological complications affect 19.4% of the patients [14]. The biochemical parameters are usually normal, including serum calcium, phosphonium, and bone turnover markers. We previously reported that two patients had elevated serum SOST levels, but the mechanism is unclear [18].

Herein, the clinical manifestations, disease-causing mutations, treatment, and follow-up of several patients were analyzed and summarized to improve the understanding of these two diseases.

Materials and methods

Subjects

This protocol was approved by the Ethics Committee of the Shanghai Sixth People's Hospital Affiliated to Shanghai Jiao Tong University School of Medicine. Written informed consents were obtained from all the subjects or their guardians. Four female and two male patients aged 6 to 64 from five families were enrolled in the present study (Fig. 1).

Clinical features and biochemical and radiographic examination evaluation

Physical examination of the patients was performed, and detailed medical histories were recorded.

Biochemical parameters, including routine blood test, serum levels of calcium (Ca), phosphonium (P), alkaline phosphatase (ALP), liver and kidney functions, creatine kinase (CK) and its MB isoenzyme (CK-MB), 25-hydroxyvitamin D [25(OH)D], the intact parathyroid hormone (PTH), the bone formation marker serum osteocalcin (OC), and the bone resorption marker serum beta cross-linked C-terminal telopeptide of type 1 collagen (β-CTX), were measured individually. Normal reference of ALP, Ca, and P [19] and normal reference of OC and β-CTX [20] for children involved in the study are listed separately.

The radiographic examinations, including X-rays of the skull, thoracolumbar, and pelvic, were performed in six patients.

Bone mineral density (BMD) was measured by a lunar prodigy dual energy X-ray absorptiometry (DXA) densitometer (Lunar Corp, Madison, WI, USA), including the anteroposterior lumbar spine 1–4 (L1-4), the left proximal femur, and the femoral neck and total hip. These data were analyzed using Prodigy enCORE software (ver. 6.70 standard-array mode; GE Healthcare, Madison, WI, USA). The Z-scores (the number of standard deviations from the mean value for persons in the general population matched for age, sex, and
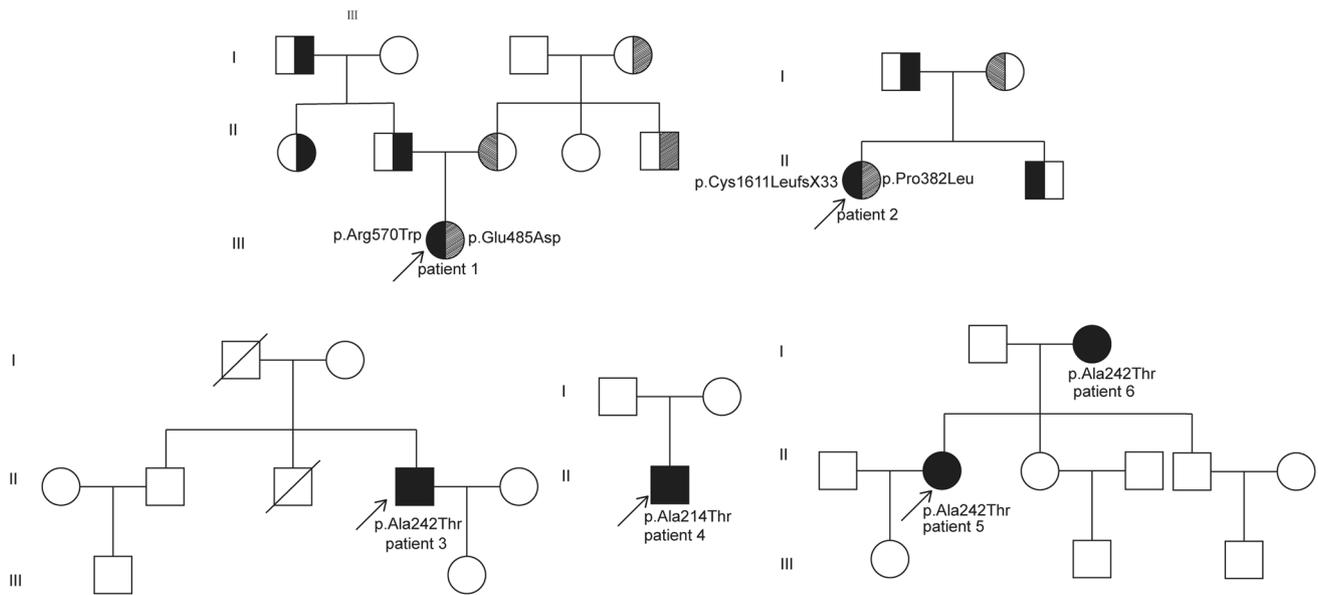
Fig. 1 Pedigree of the two OPPG and three LRP5-HBM affected families in this study

race) were used for children, premenopausal women, and men under age 50.

Genetic analysis and variant prediction

Sanger sequencing was used to detect *LRP5* mutations. Genomic DNA was extracted from the 3-mL peripheral blood sample of each participant using phenol extraction and isopropanol precipitation. Sanger sequencing was performed on patients and their family members by BigDye Terminator Cycle Sequencing Ready Reaction Kit v. 3.1 (Applied Biosystems, Foster City, CA, USA) on an ABI 3730XL automated sequencer (Thermo Fisher Scientific, Waltham, MA, USA). The sequencing files were analyzed by PolyPhred software for checking single-nucleotide polymorphisms (SNPs). The results were obtained after manual proofreading. All variants were mapped on transcript NM_002335.2 and protein NP_002326.2.

The ExAC and 1000 Genomes Project databases were used to identify the novel variant. Its amino acid conservation and pathogenicity were analyzed by UniProt databases (https://www.uniprot.org/), PolyPhen-2 (http://provean.jcvi.org), and MutationTaster (https://www.mutationtaster.org/).

Structural analysis of LRP5 protein

The protein sequence of LRP5 was obtained from the UniProt database (https://www.uniprot.org/) as a FASTA file. Three-dimensional structure homology modeling and visualization of the native and mutant proteins were performed using AlphaFold software (https://alphafold.ebi.ac.uk/) and Rosetta.

Results

OPPG

Clinical manifestation

Patient 1 Patient 1 (P1) was a 9-year-old girl born at full-term with healthy non-consanguineous parents. Her psychomotor development was normal. She was congenitally blind. The visual problems were noted at 3 months of age, showing right cataract and left microphthalmia in the ophthalmologic findings (Fig. 2a). At the age of 9, she had back pain and developed a kyphosis after falling. Radiologic examination showed significant systemic osteoporosis, increased dorsal kyphosis, and multiple vertebral compression fractures (Fig. 3a). BMD value of L1-4 was 0.363 g/cm^2, which was significantly lower than the normal range for children of the same age and gender [21]. Results of biochemical parameters were mainly within the normal range, except for the deficiency of 25(OH)D (Table 1). Concurrently, ophthalmic reexamination showed that there was an absence of bilateral optic nerve.

Patient 2 Patient 2 (P2) was the first child born to non-consanguineous parents. She was born blind and was diagnosed with right retinoblastoma and left retinal atrophy. At the age
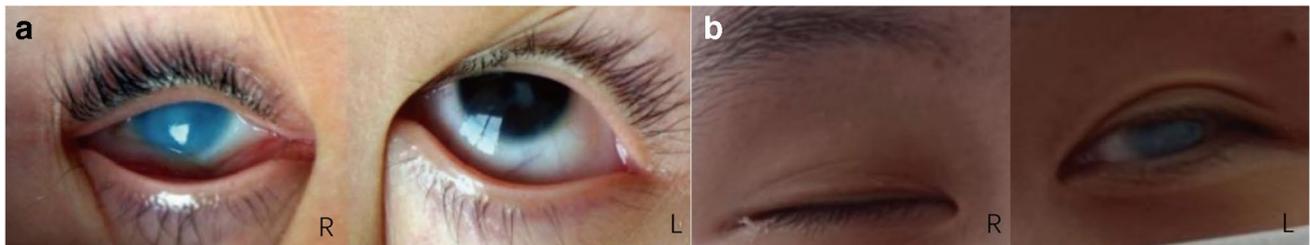
Fig. 2 Ocular clinical features of patients with OPPG. **a** Cataract (right) and microphthalmia(left). **b** Enucleation of eyeball (right) and cataract (left)
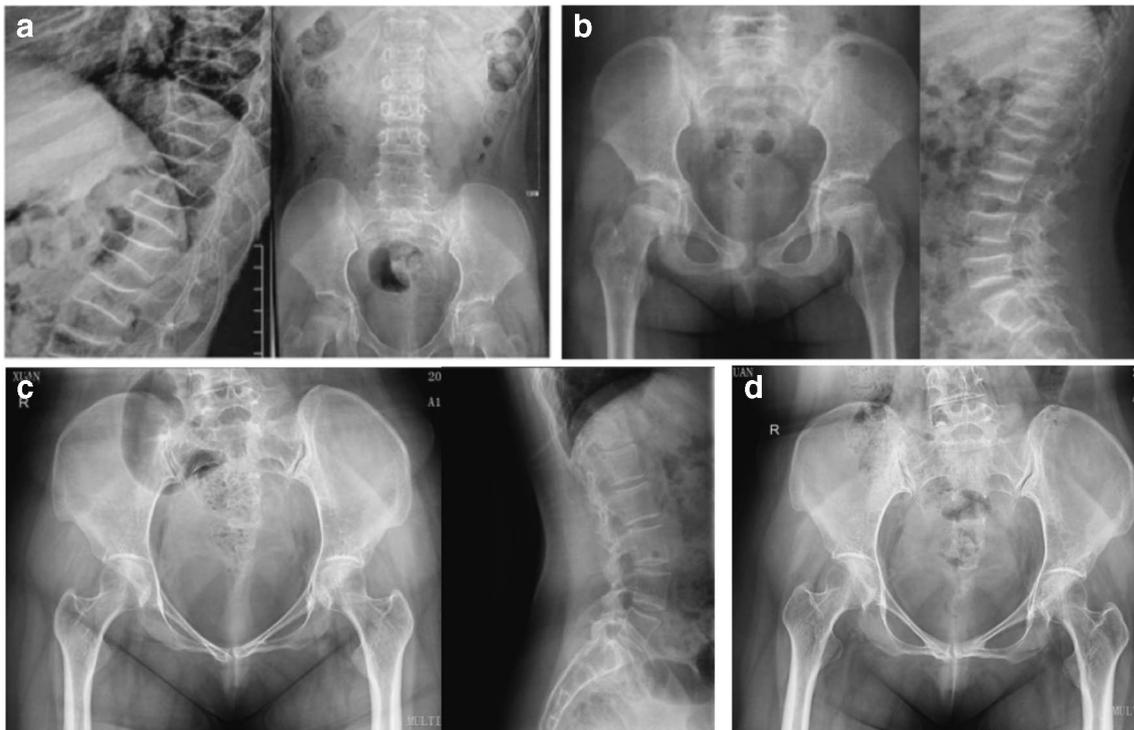

Fig. 3 X-rays of the spine and pelvic of OPPG. **a** Generalized osteoporosis with fish mouth vertebra of patient 1 before treatment. **b** Improvement of lumbar vertebral body morphology and increased BMD of patient 1 after 3-year alendronate treatment. **c** Generalized osteoporosis with lumbar scoliosis of patient 2 before treatment and **d** after 6-month zoledronate treatment

of 13, she underwent enucleation of her left eye due to tumor swelling and retinal perforation (Fig. 2b). She experienced chronic systemic bony pain and had her first nontraumatic fracture at the manubrium sterni at the age of 9. In the following years, many fractures occurred, including the ribs, humerus, thoracolumbar spine, hip, femur, tibia, and ankle, mainly involving long bones and vertebrae. When she was 16, she could not keep her upper body upright due to multiple vertebral compression fractures. She could stand unsupported but unable to walk independently and must rely on a wheelchair. In addition, she had torn ligaments in her knees and ankles and was also troubled by recurrent aseptic inflammation of her sacroiliac joint.

Besides, she has had frequent premature beats since childhood and developed into paroxysmal atrial fibrillation a few years later, and once had a cardiac arrest. However, no organic lesions were found by cardiac examination.

The results of biochemical parameters including serum calcium, phosphonium, ALP, PTH, and bone turnover markers were summarized in Table 1. Except vitamin D deficiency, all indicators were within the normal range. Radiologic examination showed thoracolumbar scoliosis, mild compression fractures of the local thoracic spine, and low pelvic BMD (Fig. 3c). The BMD of L1-4 was 0.630 g/cm^2, and the Z-score value was − 4. Her parents and brother were healthy and had no vision or skeletal problems.

Table 1 Baseline clinical features and bone mineral density in affected patients

	Patient 1 (OPPG)	Patient 2 (OPPG)	Patient 3 (LRP5-HBM)	Patient 4 (LRP5-HBM)	Patient 5 (LRP5-HBM)	Patient 6 (LRP5-HBM)
Gender/age (years)	F/9	F/27	M/32	M/6	F/40	F/64
Height (cm)	137	152	187	124	173	167
Fragility fracture	Yes	Yes	No	No	No	No
Bone pain	Yes	Yes	Yes	No	Yes	Yes
Skeletal deformity	Kyphosis	Scoliosis	Torus palatinus	Thoracic deformity	Torus palatinus, elongated mandible	Torus palatinus, elongated mandible
Ocular involvement	Cataract, microphthalmia	Retinoblastoma, retinal atrophy	No	No	No	No
Hearing loss	No	No	No	No	No	No
Cognitive impairment	No	No	No	No	No	No
ALP (U/L)	219.9 (116–380)[a]	96	62	268 (116–380)[a]	60	115*
Ca (mmol/L)	2.55 (2.25–2.75)[a]	2.32	2.35	2.43 (2.25–2.75)[a]	2.39	2.11
P (mml/L)	1.65 (1.29–1.94)[a]	1.31	0.73	1.42 (1.29–1.94)[a]	1.24	1.56
β-CTX (ng/L)	1160 (610–1980)[b]	190.3	403.6	1707 (950–2190)[b]	140	1500*
OC (ng/mL)	96.53 (46.0–129.2)[b]	17.74	21.73	92.63 (49.5–137.8)[b]	NA	NA
25(OH)D (ng/mL)	11.98*	10.38*	35.98	34.98	9.66*	11.33*
PTH (pg/mL)	44.07	26.17	46.17	43.51	25.51	20.35
L1-L4 BMD (g/cm^2)	0.363	0.630 (Z: − 4.0)	2.360 (Z: 10.5)	1.149	2.016 (Z: 5.5)	1.930 (T: 6.5)
FN BMD (g/cm^2)	0.34	0.562 (Z: − 3.1)	2.431 (Z: 11.1)	1.327	2.030 (Z: 7.9)	1.455 (T: 4.4)
TH BMD (g/cm^2)	0.377	0.603 (Z: − 2.9)	2.596 (Z: 12.3)	1.321	2.104 (Z: 7.6)	1.505 (T: 4.1)

Notes: Values marked with asterisk (*) indicate the levels of markers were beyond the normal range; "NA" means not available

Reference range: ALP: 15–112 U/L; Ca: 2.08–2.6 mmol/L; P: 0.8–1.6 mmol/L; β-CTX: 112–497 ng/mL for female, 100–612 ng/ml for male; OC: 4.91–22.31 ng/mL for female, 5.58–28.62 ng/mL for male; PTH: 15–65 pg/ml; 25(OH)D: > 20 ng/mL

BMD bone mass density, *F* female, *M* male, *ALP* alkaline phosphatase, *Ca* calcium, *P* phosphate, *OC* osteocalcin, *PTH* parathyroid hormone, *β-CTX* β-isomerized C-terminal cross-linked telopeptide of type I collagen, *25(OH)D* 25-hydroxyvitamin D, *FN* femoral neck, *TH* total hip

[a]Reference for children

[b]Reference for girls and boys between the ages of 6 and 9 years

Identification of LRP5 variants

We verified the mutations in the patients and their family members if they agreed, and the results are presented in Figs. 1a, b and 6a. Sanger sequencing confirmed that P1 had a compound heterozygous mutation in exon 7 (c.1455G > T, p.Glu485Asp) and exon 8 (c.1708C > T, p.Arg570Trp) and P2 had a compound heterozygous mutation in exon 6 (c.1145C > T, p.Pro382Leu) and exon 23 (c.4830dupC, p.cys1611leufsx33). Meanwhile, some healthy relatives of the two patients carried a heterozygous mutation from their corresponding family.

Variant prediction and structural analysis

Multiple sequence alignment reveals that Glu485 is highly conserved in different species (Fig. 6a), and Glu485Asp is predicted as "disease-causing" by PolyPhen-2, MutationTaster, SIFT, and PROVEAN (Supplementary table). Furthermore, the three-dimensional structure homology modeling and visualization of the native and the three missense mutant proteins show that the three mutations have no apparent effect on protein structure. As for Pro382Leu, since no hydrogen bonds are formed before and after the mutation, there are no changes at least in the hydrogen bonds formed with neighboring atoms at the mutation site. However, as for Glu485Asp, our AlphaFold result shows there are changes in the length of the hydrogen bonds, while Rosetta result shows the number of hydrogen bonds changed from four in the native type to two in the mutant type. It also forms fewer hydrogen bonds at the site of the Arg570Trp in both modeling results (Fig. 6b and SI).

Treatment and follow-up

P1 received oral alendronate treatment at a dose of 70 mg/week from the age of 9 to 12. During the 3-year treatment, bone pain was significantly relieved. The baseline and follow-up serum levels of calcium, phosphorus, bone turnover markers, alkaline phosphatase, and PTH were summarized in Table 2. All of them were within in the normal level and showed no significant difference. Oral administration of 600 IU of vitamin D3 per day did not improve the state of vitamin D deficiency. The spinal X-ray after treatment showed significant improvement in the shape of the thoracolumbar spine (Fig. 3b), and there were no new fractures during the treatment. Furthermore, the BMD of L1-4, femur neck, and total hip was significantly increased by 107.2%, 70.0%, and 65.5%, respectively (Table 2).

As for P2, she was diagnosed as "osteoporosis" or "osteogenesis imperfecta" in other hospitals and took alendronate 70 mg per week at the age of 13. Six months later, she quit because of recurrence of fractures and no significant improvement in BMD. Last year, at the age of 27, she received 5 mg of zoledronic acid intravenously. Simultaneously, she took vitamin D3 800 IU and calcium 1000 mg per day. The clinical symptoms improved within half a year after injection. She could walk longer without a wheelchair. Although she fell down twice, she did not have a fracture, which was likely to happen in the past. BMD of L1-4, femoral neck, and total hip increased by 5.87%, 6.76%, and 4.15%, and β-CTX and osteocalcin decreased slightly after 6 months of treatment. Serum calcium, phosphorus, and parathyroid hormone levels were almost unchanged. Although the level of 25(OH)D increased, it was still below the normal range (Table 2).

No serious adverse drug reactions occurred in both patients during the treatment.

LRP5-HBM

Clinical manifestations

Patient 3 Patient 3 (P3), a 32-year-old male, came to our department because of lumbodorsal pain. A torus palatinus in the center of the oral hard palate was detected by physical examination (Fig. 4a). X-ray examination revealed that the skull, thoracolumbar vertebrae, and pelvis bones were dense, and the cranial plate was significantly thickened (Fig. 5a). The Z-scores of BMD of the L1-4, femur neck, and total hip were + 10.5, + 11.1, and + 12.3, respectively (Table 1). The patients have no history of fractures, sensorimotor neuropathy, and visual or hearing impairment. The level of serum calcium, phosphonium, ALP, PTH, 25(OH)D,

Table 2 Pre- and post-treatment biochemical data and bone mineral density of two OPPG patients

Index	ALP (U/L)	Ca (mmol/L)	P (mml/L)	β-CTX (ng/L)	OC (ng/mL)	25(OH)D (ng/mL)	PTH (pg/mL)	BMD (g/cm²)		
								L1-L4	FN	TH
Patient 1										
Pre-treatment	219.9 (116–380)[a]	2.55 (2.25–2.75)[a]	1.65 (1.29–1.94)[a]	1160 (610–1980)[b]	96.53 96.53 (46.0–129.2)[b]	11.98*	44.07	0.363	0.34	0.377
Post-treatment (3Y)	157 (116–380)[a]	2.48 (2.25–2.75)[a]	1.39 (1.29–1.94)[a]	1243 (390–2370)[b]	87.05 (19.2–205.2)[b]	12.43*	50.90	0.752	0.578	0.624
Patient 2										
Pre-treatment	96	2.32	1.31	190.3	17.74	10.38*	26.17	0.630	0.562	0.603
Post-treatment (6 M)	84	2.33	1.32	101.80	9.41	11.50*	18.76	0.667	0.600	0.628

Notes: Values marked with asterisk (*) indicate the levels of markers were beyond the normal range; "NA" means not available

Reference range: ALP: 15–112 U/L; Ca: 2.08–2.6 mmol/L; P: 0.8–1.6 mmol/L; β-CTX: 112–497 ng/mL for female; PTH: 15–65 pg/mL; 25(OH)D: >20 ng/mL

3Y 3 years, *6 M* 6 months, *BMD* bone mass density, *F* female, *M* male, *ALP* alkaline phosphatase, *Ca* calcium, *P* phosphate, *OC* osteocalcin, *PTH* parathyroid hormone, *β-CTX* β-isomerized C-terminal cross-linked telopeptide of type I collagen, *25(OH)D* 25-hydroxyvitamin D, *FN* femoral neck, *TH* total hip

[a]Reference for children

[b]Reference for girls between the ages of 9 and 12 years
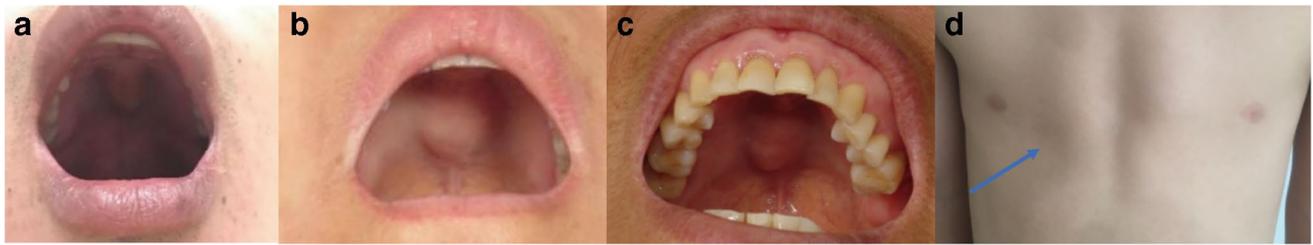
Fig. 4 Clinical manifestations of patients with LRP5-HBM. **a**, **b**, **c** The torus palatinus in the center of the hard palate of 3 patients. **d** A slight depression in the right chest of patient 4
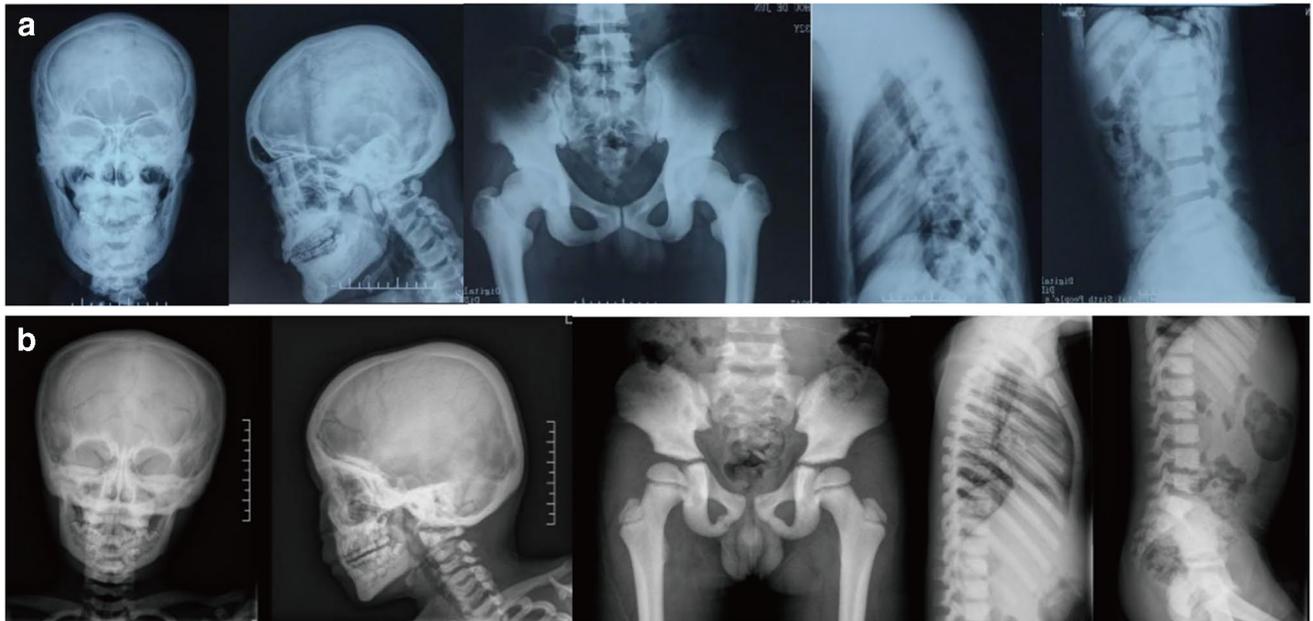

Fig. 5 X-rays of the skull, spine, humerus, and femur of two LRP5-HBM patients (**a**: patient 3; **b**: patient 4). Osteosclerosis of the skull with an enlarged sella turcica. Generalized osteosclerosis. Cortical thickening of the humerus and femur with a normal external shape

and bone turnover markers was all within the normal range (Table 1). His family members were all healthy.

Patient 4 Patient 4 (P4) was a 6-year-old boy born at full-term who was found to have thoracic deformity at the age of 3. He was diagnosed as "Rickets" in the local hospital, but the symptoms did not improve after calcium and vitamin D supplementation. At the age of 6, the abnormal increased bone mineral density of ribs, sternum, thoracic vertebrae, and bilateral humeral metaphysis was identified by occasionally chest X-ray examination due to cough. In order to confirm the diagnosis, the child underwent further radiological examination. The examination found that the patient's whole-body BMD increased and the skull plate thickened (Fig. 5b). The patient had normal tooth development and maxillary morphology. No jaw enlargement or palatal ring

was found. The patient had a slight depression on the right side of the chest (Fig. 4d) and had no history of fracture.

Moreover, the value of BMD of L1-4, femoral neck, and total hip was 1.149 g/cm^2, 1.327 g/cm^2, and 1.321 g/cm^2, respectively (Table 1). The biochemical indices including serum calcium and phosphonium, ALP, PTH, 25(OH)D, β-CTX, and OC were within the normal range (Table 1).

His parents were healthy and non-consanguineous.

Patients 5 and 6 Patients 5 (P5) and 6 (P6) were a mother-daughter pair, as reported in our previous study [18]. In brief, both of them had chronic lumbodorsal pain, an elongated mandible and torus palatinus (Fig. 4b and c), high bone mass, but no history of fractures. X-ray radiographs showed thickening of the cranial plates, an elongated mandible, cortical thickening of the long bones, and degenerative
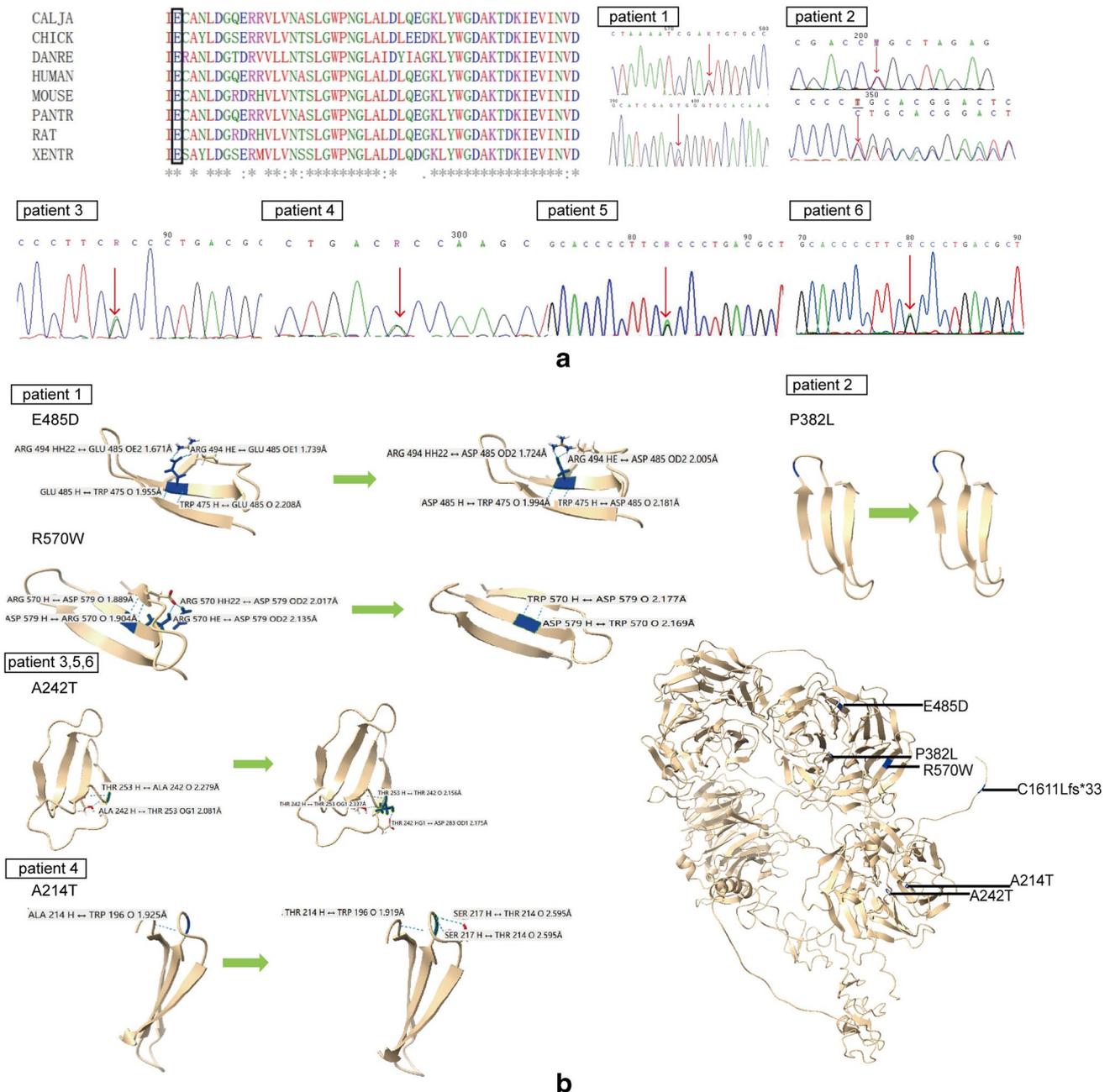
Fig. 6 Sanger sequencing and the three-dimensional modeling. **a** Multiple sequence alignments revealed that the glu485 residue in the LRP5 protein was highly conserved among species; Sanger sequencing of the LRP5 mutations: p.Glu485Asp (E485D, c.1455G > T) and p.Arg570Trp (R570W, c.1708C > T) in patient 1; p.Pro382Leu (P382L, c.1145C > T) and p.Cys1611LeufsX33 (c.4830dupC) in patient 2; p.Ala242Thr (A242T, c.724G > A) in patients 3, 5, and 6; p.Ala214Thr (A214T, c.640G > A) in patient 4. **b** Comparison of the three-dimensional modeling of wild and missense mutations' local structures by AlphaFold; distribution of the six mutation sites on the LRP5 protein

changes. The biochemical indices showed that they both had vitamin D deficiency. The serum ALP level of patient 6 was slightly higher than normal range, while β-CTX was much higher than the normal range (Table 1).

Identification of LRP5 variants

The *LRP5* gene detection results of patients and their family members were shown in Figs. 1c, d, and e and 6a. By Sanger

sequencing, the heterozygous c.724G > A (p.Ala242Thr) mutation was detected in P3, P5, and P6. And the heterozygous c.640G > A (p.Ala214Thr) mutation was detected in P4. We did not identify any pathogenic variants in family members other than the patients.

Structural analysis

As predicted by AlphaFold and Rosetta, the conversion of alanine to threonine in two mutation sites has no apparent effect on protein structure. But in the modeling results of both software, the number of hydrogen bonds increases after the mutations (Fig. 6b and SI).

Follow-up

P5 underwent 12 years of follow-up. During the follow-up period, pain in the thoracolumbar spine, cervical spine, and shoulders was the main issue, but there were no fractures, no dental problems, and no significant changes in height. In addition, no neurological symptoms such as trigeminal neuralgia, neurogenic hearing loss, visual field deficits, or chronic headaches occurred during the follow-up period. She only takes painkillers when necessary to relieve her lower back pain. In the past year, she has experienced menstrual cycle disorders. After 12 years of diagnosis, the patient underwent a reexamination of BMD, bone turnover markers, and biochemical parameters. The detailed results were summarized in Table 3. Compared with the results 12 years ago, the absolute value of BMD of L1-4, femoral neck, and total hip was decreased by 9.62%, 12.81%, and 11.03%, respectively, but it was still higher than the reference value of the same age and gender. The serum levels of PTH, Ca, and P were normal, but 25(OH)D is still below the normal range. Bone turnover markers, including β-CTX and OC, were higher than the normal range.

Discussion

In the current study, we reported five mutations and a variant, four from OPPG patients (Glu485Asp, Arg570Trp, Pro382Leu and Cys1611LeufsX33) and two from LRP5-HBM patients (Ala242Thr and Ala214Thr). Glu485Asp, Arg570Trp, and Pro382Leu all lie in the exons collectively coding for the second β-propeller domain, consistent with that most OPPG mutations reported have been described in the second and third b-propeller domains [22]. However, Cys1611LeufsX33 lies in the intracellular domain, which is supposed to be phosphorylated and therefore inhibit GSK3b when Wnts bind to its coreceptors Frizzled and LRP6/5 [23]. In addition, the novel variant Glu485Asp is considered to

Table 3 Baseline and follow-up data of biochemical data and bone mineral density of one LRP5-HBM patient (Patient 5)

Index	ALP (U/L)	Ca (mmol/L)	P (mml/L)	β-CTX (ng/L)	OC (ng/mL)	25(OH)D (ng/mL)	PTH (pg/mL)	BMD (g/cm^2) (Z-score)		
								L1-L4	FN	TH
Baseline	60	2.39	1.24	140	NA	9.66*	25.51	2.016 (5.5)	2.030 (7.9)	2.104 (7.6)
After 12Y	122*	2.33	1.18	759.70*	30.53*	12.82*	28.11	1.822 (6.6)	1.770 (7.7)	1.872 (7.4)

Notes: Values marked with asterisk (*) indicate the levels of markers were beyond the normal range; "NA" means not available

Reference range: ALP: 15–112 U/L; Ca: 2.08–2.6 mmol/L; P: 0.8–1.6 mmol/L; β-CTX: 112–497 ng/mL for female, 100–612 ng/mL for male; OC: 4.91–22.31 ng/mL for female, 5.58–28.62 ng/mL for male; PTH: 15–65 pg/mL; 25(OH)D: > 20 ng/mL

12Y 12 years, *BMD* bone mass density, *F* female, *M* male, *ALP* alkaline phosphatase, *Ca* calcium, *P* phosphate, *OC* osteocalcin, *PTH* parathyroid hormone, *β-CTX* β-isomerized C-terminal cross-linked telopeptide of type I collagen, *25(OH)D* 25-hydroxyvitamin D, *FN* femoral neck, *TH* total hip

be pathogenic after conservation and pathogenicity prediction, which broadens the variation spectrum of pathogenic genes. Ala242Thr and Ala214Thr are the hot spot mutations in patients with LRP5-HBM [3, 14, 18], both located in the amino terminal part of the gene, before the first EGF-like domain, like the previously reported mutations that cause the high-bone-mass phenotype. Besides, Ala242Thr has been predicted to incline to disrupt the core packing of the LRP5 protein structure and affect the first β-propeller domain, thereby destabilizing the binding site of SOST and LRP5 [24]. We performed the three-dimensional structure homology modeling and visualization of the native and five missense mutant proteins using the online AlphaFold and Rosetta software. Glu485Asp, Arg570Trp, Ala214Thr, and Ala242Thr all had variations in the number or length of hydrogen bonds. Interestingly, we found that the number of hydrogen bonds at the mutation site decreased in the loss-of-function mutation (Glu485Asp and Arg570Trp), while they increased in the gain-of-function mutation (Ala214Thr and Ala242Thr), which may be associated with the loss and gain of LRP5 function. Modeling of Pro382Leu by two software showed no significant changes in structure and hydrogen bonding before and after mutation, but case reports of both homozygous and compound heterozygous mutations of Pro382Leu have been reported [25, 26]. Its effect on the local structure of LRP5 protein and the intensity of Wnt signaling pathway remained unclear. Cys1611LeufsX33 was a frameshift mutation where termination codon was shifted back. And the mutation was located at the site where LRP5 intracellular structure binds to Wnts and Frizzled, which might have a great influence on the transmission of the intracellular part of Wnt signal.

OPPG children may sometimes be misdiagnosed as osteogenesis imperfecta, but they have no identifiable defects in collagen synthesis and metabolism, with their calcium homeostasis, endochondral growth, and bone turnover index all normal [27, 28]. It is worth mentioning that P2 has developed nonorganic paroxysmal atrial fibrillation of unknown cause in recent years, which is not found in other OPPG patients reported. Besides, neurological diseases such as seizures, autism spectrum disorder, and intellectual deficit in individual OPPG cases are reported abroad [29–31], but there are not such problems in OPPG patients reported in our country [32], including the two patients in present study. It is still unclear whether the clinical variability of neurological phenotypes can be attributed to mutational effects or a specific protein domain [10, 33].

At present, there are few treatment options for OPPG children. Bisphosphonates are the most commonly used and rational drug for them, and its effect on improving the bone condition has been confirmed [9, 30]. In the present study, the beneficial effects have been observed in the 3-year alendronate sodium for P1 and half-year intravenous zoledronic acid for P2. During and after bisphosphonate treatment, for both the biochemical indexes and hormone values were basically within the normal range, the symptoms were improved, and the risk of fracture was reduced. However, P2 experienced a period of failed oral alendronate treatment before the zoledronic acid, manifested by the appearance of new fractures and unrelieved bone pain. Actually, in this case, the drug adjustment should be determined according to a combination of factors, including fracture history, bone pain, growth, and bone mineral density.

In the present study, high bone mass, torus palatinus, and an elongated mandible were the most common clinical symptoms for our LRP5-HBM patients. The serum ALP of all patients was within the normal range, and no symptoms of nervous system were involved. Interestingly, the 6-year-old patient (P4) did not have torus palatinus but had thoracic deformity, which had never been reported in cases of LRP5-HBM, and it was uncertain whether it was caused by *LRP5* gene mutation.

In the current study, we found that P5 has entered a period of rapid bone turnover; β-CTX and OC were out of normal range. The BMD of L1-4 decreased by 9.6% within 12 years, with an average annual decrease of 0.8%. Considering that our patient has been in the late perimenopause stage (no menstrual bleeding in the last 3 months but some menstrual bleeding during the last 11 months), the menstrual disorder in the past year may partly be the reason for the decrease of bone mass and the acceleration of bone turnover. Since there were no long-term longitudinal studies on changes in bone mineral density during the perimenopausal transition in mainland Chinese women, we used data collected from women in Chinese Hong Kong [34] as a reference, from which we estimated that the lumbar spine bone loss rate of healthy women population from age 40 to 52 is about 7.94%. Anyhow, it seemed that our patient did not seem to lose bone at a slower rate than healthy controls, and the gain-of-function mutation Ala242Thr could not protect her from age-related and estrogen-related bone loss. Similarly, another study found that individuals with LRP5$_{T253I}$-HBM were not protected from age-related bone loss, at least at the hip and femoral neck [35]. Whether *LRP5* gain-of-function mutations can actually help carriers resist bone loss due to bone wasting factors, and whether this effect is related to the mutation site needs more follow-up data to be confirmed.

Conclusion

In the current study, two cases of OPPG caused by *LRP5* loss-of-function mutations and four cases of LRP5-HBM caused by *LRP5* gain-of-function mutations were reported. For OPPG, a novel heterozygous missense mutation was reported to expand the genotypic spectrum of OPPG. The

bisphosphonates treatment can increase the BMD and decrease the risk of fracture for patients with OPPG. On the other hand, LRP5-HBM is a relatively benign disease. *LRP5* gene mutation, however, may not slow down the rate of bone loss, including postmenopausal bone loss. This phenomenon deserves further observation and study.

Declarations

Consent to Participate Written informed consent was obtained from the patient to publish this case report and any accompanying images.

Conflicts of interest None.

References

1. Hussain MM, Strickland DK, Bakillah A (1999) The mammalian low-density lipoprotein receptor family. Annu Rev Nutr 19:141–172
2. Baron R, Rawadi G, Roman-Roman S (2006) Wnt signaling: a key regulator of bone mass. Curr Top Dev Biol 76:103–127
3. Van Wesenbeeck L, Cleiren E, Gram J, Beals RK, Bénichou O, Scopelliti D et al (2003) Six novel missense mutations in the LDL receptor-related protein 5 (LRP5) gene in different conditions with an increased bone density. Am J Hum Genet 72(3):763–771
4. Baron R, Kneissel M (2013) WNT signaling in bone homeostasis and disease: from human mutations to treatments. Nat Med 19(2):179–192. https://doi.org/10.1038/nm.3074
5. Balemans W, Piters E, Cleiren E, Ai M, Van Wesenbeeck L, Warman ML et al (2008) The binding between sclerostin and LRP5 is altered by DKK1 and by high-bone mass LRP5 mutations. Calcif Tissue Int 82(6):445–453. https://doi.org/10.1007/s00223-008-9130-9
6. Gong Y, Slee RB, Fukai N, Rawadi G, Roman-Roman S, Reginato AM et al (2001) LDL receptor-related protein 5 (LRP5) affects bone accrual and eye development. Cell 107(4):513–523
7. Boyden LM, Mao J, Belsky J, Mitzner L, Farhi A, Mitnick MA et al (2002) High bone density due to a mutation in LDL-receptor-related protein 5. N Engl J Med 346(20):1513–1521
8. Patel MS, Karsenty G (2002) Regulation of bone formation and vision by LRP5. N Engl J Med 346(20):1572–1574
9. Zacharin M, Cundy T (2000) Osteoporosis pseudoglioma syndrome: treatment of spinal osteoporosis with intravenous bisphosphonates. J Pediatr 137(3):410–415
10. Ai M, Heeger S, Bartels CF, Schelling DK (2005) Clinical and molecular findings in osteoporosis-pseudoglioma syndrome. Am J Hum Genet 77(5):741–753
11. Levasseur R, Lacombe D, de Vernejoul MC (2005) LRP5 mutations in osteoporosis-pseudoglioma syndrome and high-bone-mass disorders. Joint Bone Spine 72(3):207–214
12. Lee DH, Wenkert D, Whyte MP, Trese MT, Cruz OA (2003) Congenital blindness and osteoporosis-pseudoglioma syndrome. J AAPOS 7(1):75–77
13. Gorlin RJ, Glass L (1977) Autosomal dominant osteosclerosis. Radiology 125(2):547–548
14. De Mattia G, Maffi M, Mosca M, Mazzantini M (2023) LRP5 high bone mass (Worth-type autosomal dominant endosteal hyperostosis): case report and historical review of the literature. Arch Osteoporos 18(1):112. https://doi.org/10.1007/s11657-023-01319-6
15. Lapresle J, Maroteaux P, Kuffer R, Said G, Meyer O (1976) Dominant generalized cortical hyperostosis with multiple involvement of the cranial nerves. Nouv Presse Med 5(40):2703–2706
16. Adès LC, Morris LL, Burns R, Haan EA (1994) Neurological involvement in Worth type endosteal hyperostosis: report of a family. Am J Med Genet 51(1):46–50
17. Perez-Vicente JA, Rodríguez de Castro E, Lafuente J, Mateo MM, Giménez-Roldán S (1987) Autosomal dominant endosteal hyperostosis. Report of a Spanish family with neurological involvement. Clin Genet 31(3):161–9
18. Wang C, Zhang B-H, Zhang H, He J-W, Hu Y-Q, Li M et al (2013) The A242T mutation in the low-density lipoprotein receptor-related protein 5 gene in one Chinese family with osteosclerosis. Intern Med 52(2):187–192
19. Rauchenzauner M, Schmid A, Heinz-Erian P, Kapelari K, Falkensammer G, Griesmacher A et al (2007) Sex- and age-specific reference curves for serum markers of bone turnover in healthy children from 2 months to 18 years. J Clin Endocrinol Metab 92(2):443–449
20. Huang Y, Eapen E, Steele S, Grey V (2011) Establishment of reference intervals for bone markers in children and adolescents. Clin Biochem 44(10–11):771–778. https://doi.org/10.1016/j.clinbiochem.2011.04.008
21. Zhu H, Fang J, Luo X, Yu W, Zhao Y, Li X et al (2010) A survey of bone mineral density of healthy Han adults in China. Osteoporos Int 21(5):765–772. https://doi.org/10.1007/s00198-009-1010-2
22. Rickels MR, Zhang X, Mumm S, Whyte MP (2005) Oropharyngeal skeletal disease accompanying high bone mass and novel LRP5 mutation. J Bone Miner Res 20(5):878–885
23. Piao S, Lee S-H, Kim H, Yum S, Stamos JL, Xu Y et al (2008) Direct inhibition of GSK3beta by the phosphorylated cytoplasmic domain of LRP6 in Wnt/beta-catenin signaling. PLoS ONE 3(12):e4046. https://doi.org/10.1371/journal.pone.0004046
24. Gregson CL, Wheeler L, Hardcastle SA, Appleton LH, Addison KA, Brugmans M et al (2016) Mutations in known monogenic high bone mass loci only explain a small proportion of high bone mass cases. J Bone Miner Res 31(3):640–649. https://doi.org/10.1002/jbmr.2706
25. Astiazarán MC, Cervantes-Sodi M, Rebolledo-Enríquez E, Chacón-Camacho O, Villegas V, Zenteno JC (2017) Novel homozygous LRP5 mutations in Mexican patients with osteoporosis-pseudoglioma syndrome. Genet Test Mol Biomarkers 21(12):742–746. https://doi.org/10.1089/gtmb.2017.0118

26. Narumi S, Numakura C, Shiihara T, Seiwa C, Nozaki Y, Yamagata T et al (2010) Various types of LRP5 mutations in four patients with osteoporosis-pseudoglioma syndrome: identification of a 7.2-kb microdeletion using oligonucleotide tiling microarray. Am J Med Genet A 152A(1):133–40. https://doi.org/10.1002/ajmg.a.33177

27. Levasseur R (2008) Treatment and management of osteoporosis-pseudoglioma syndrome. Expert Rev Endocrinol Metab 3(3):337–348. https://doi.org/10.1586/17446651.3.3.337

28. Teebi AS, Al-Awadi SA, Marafie MJ, Bushnaq RA, Satyanath S (1988) Osteoporosis-pseudoglioma syndrome with congenital heart disease: a new association. J Med Genet 25(1):32–36

29. Laine CM, Chung BD, Susic M, Prescott T, Semler O, Fisker-strand T et al (2011) Novel mutations affecting LRP5 splicing in patients with osteoporosis-pseudoglioma syndrome (OPPG). Eur J Hum Genet 19(8):875–881. https://doi.org/10.1038/ejhg.2011.42

30. Karakilic-Ozturan E, Altunoglu U, Ozturk AP, Kardelen Al AD, Yavas Abali Z, Avci S et al (2022) Evaluation of growth, puberty, osteoporosis, and the response to long-term bisphosphonate therapy in four patients with osteoporosis-pseudoglioma syndrome. Am J Med Genet A 188(7):2061–2070. https://doi.org/10.1002/ajmg.a.62742

31. Welinder LG, Robitaille JM, Rupps R, Boerkoel CF, Lyons CJ (2015) Congenital bilateral retinal detachment in two siblings with osteoporosis-pseudoglioma syndrome. Ophthalmic Genet 36(3):276–280. https://doi.org/10.3109/13816810.2015.1016240

32. Bai Z, Jiao Z, Kong X (2022) Analysis of LRP5 gene variants in a Chinese pedigree affected with osteoporosis-pseudoglioma syndrome. Zhonghua Yi Xue Yi Chuan Xue Za Zhi 39(2):185–188. https://doi.org/10.3760/cma.j.cn511374-20201125-00828

33. Papadopoulos I, Bountouvi E, Attilakos A, Gole E, Dinopoulos A, Peppa M et al (2019) Osteoporosis-pseudoglioma syndrome: clinical, genetic, and treatment-response study of 10 new cases in Greece. Eur J Pediatr 178(3):323–329. https://doi.org/10.1007/s00431-018-3299-3

34. Tang GW, Yip PS, Li BY (2001) The profile of bone mineral density in chinese women: its changes and significance in a longitudinal study. Osteoporos Int 12(8):647–653

35. Lauterlein J-JL, Gossiel F, Weigl M, Eastell R, Hackl M, Hermann P et al (2021) Development of the bone phenotype and microRNA profile in adults with low-density lipoprotein receptor-related protein 5-high bone mass (LRP5-HBM) disease. JBMR Plus 5(9):e10534. https://doi.org/10.1002/jbm4.10534